Computational Study on the Solubility of Lithium Salts Formed on Lithium Ion Battery Negative Electrode in Organic Solvents

Ken Tasaki*,† and Stephen J. Harris‡

Mitsubishi Chemical USA, 410 Palos Verdes Boulevard, Redondo Beach, California 90277, and General Motors Corporation Research & Development Center, Mail Code 480-102-000, 30500 Mound Road, Warren, Michigan 48090

Received: January 2, 2010; Revised Manuscript Received: March 22, 2010

The solubility of lithium salts, found in solid-electrolyte interface (SEI) films on the anode surface in lithium ion battery cells, has been examined in organic solvents through atomistic computer simulations. The salts included lithium oxide (Li_2O), lithium carbonate (Li_2CO_3), lithium oxalate ($[LiCO_2]_2$), lithium fluoride (LiF), lithium hydroxide (LiOH), lithium methoxide ($LiOCH_3$), lithium methyl carbonate ($LiOCO_2CH_3$), lithium ethyl carbonate ($LiOCO_2C_2H_5$), and dilithium ethylene glycol dicarbonate (($[CH_2OCO_2Li]_2$: LiEDC). The organic solvents were dimethyl carbonate (DMC) and ethylene carbonate (EC). The atomic charges in the force field have been fitted to the electrostatic potential obtained from density functional theory calculations for each salt. The heat of dissolution in DMC for the salts calculated from computer simulations ranged from exothermic heats for the organic salts in general to endothermic heats for the inorganic salts in the order of LiEDC < $LiOCO_2CH_3$ < LiOH < $LiOCO_2C_2H_5$ < $LiOCH_3$ < LiF < $[LiCO_2]_2$ < Li_2CO_3 < Li_2O where the value of the heat went from more negative in the left to more positive in the right. In EC, the order was more or less the same, but the salts were found to dissolve more than DMC in general. The analysis from simulations was performed to rationalize the solubility of each salt in DMC and also the solubility difference between in DMC and EC. The latter was found to be due not only to the difference in polarity between the two solvents, but we also suspect that it may be due to the molecular shapes of the solvents. We also found that the conformation of LiEDC changed in going from DMC to EC, which contributed to the difference in the solubility.

The solid-electrolyte-interface (SEI) film formed on the negative electrode in lithium ion battery cells has been found to be a key component affecting important cell performance parameters, such as cycle life, calendar life, irreversible capacity loss, safety, and others.[1−35] The dissolution of the SEI film during cycling or storage has been discussed by a number of groups and has been claimed to be a major cause for capacity fading.[4,34,35] Film dissolution can result in exposure of the electrode surface to the electrolyte, prompting irreversible reactions with the electrolyte, thus reducing the cell capacity. However, most of the previous reports have been based on indirect observations of the film dissolution, such as the disappearance of differential scanning calorimetry peaks[5] and changes in the X-ray photospectroscopy spectra[13,21,26,34,35] or the atomic force microscopy images[13] before and after cycling or storage. We have recently determined the solubility of individual lithium salts typically found in the SEI film in dimethyl carbonate (DMC) through ion conductivity measurements.[36] We found that organic salts were more likely to dissolve than inorganic salts. On the basis of the results, we proposed a mechanism by which a capacity fading may be facilitated by the SEI film dissolution, but we provided little interpretation of the solubility data in our previous paper.[36]

Computer simulation may be a useful tool to interpret the experimental solubility data and gain insight into the solubility behavior of the lithium salts in organic solvents. Further, rationalization of the lithium salt solubility measurements may provide useful information for designing a stable SEI film. We report here a detailed examination of the solubility of the lithium salts using the results from computer simulations. The lithium salts studied here include lithium oxide (Li_2O), lithium carbonate (Li_2CO_3), lithium oxalate ($[LiCO_2]_2$), lithium fluoride (LiF), lithium hydroxide (LiOH), lithium methoxide ($LiOCH_3$), lithium methyl carbonate ($LiOCO_2CH_3$), lithium ethyl carbonate ($LiOCO_2C_2H_5$), and dilithium ethylene glycol dicarbonate ($[CH_2OCO_2Li]_2$, LiEDC), all of which have been found as SEI film components.[1,5,9,14−35] The solvents in which the solubility of the lithium salts was examined were DMC and ethylene carbonate (EC). This work is a series of reports in understanding SEI film solubility, which may lead to practical rejuvenation of lithium ion cells. Because the application of lithium ion batteries for transportation is expected to grow, recycling or refurbishing used cells will become an important issue.

The lithium salts studied here may fall into a category of ionic solids in materials science. Computer modeling of ionic solids has been found to be challenging due to the strong polarization effects, among other factors.[37] Still, computational modeling approaches have been successfully applied to several lithium ions, such as Li_2O[38−46] and Li_2CO_3.[47] The primary reason for such a predominantly large number of reports for Li_2O is due to its interest as an ionic conductor.[38] However, most of the studies used ad hoc force fields for particular salts. Furthermore, very few potential functions or force field parameters have been proposed for the other lithium salts examined in this study, partially due to the lack of experimental data. We

* Corresponding author. E-mail: ken_tasaki@m-chem.com.
† Mitsubishi Chemical USA.
‡ General Motors Corporation.

10.1021/jp100013h
Published on Web 04/06/2010

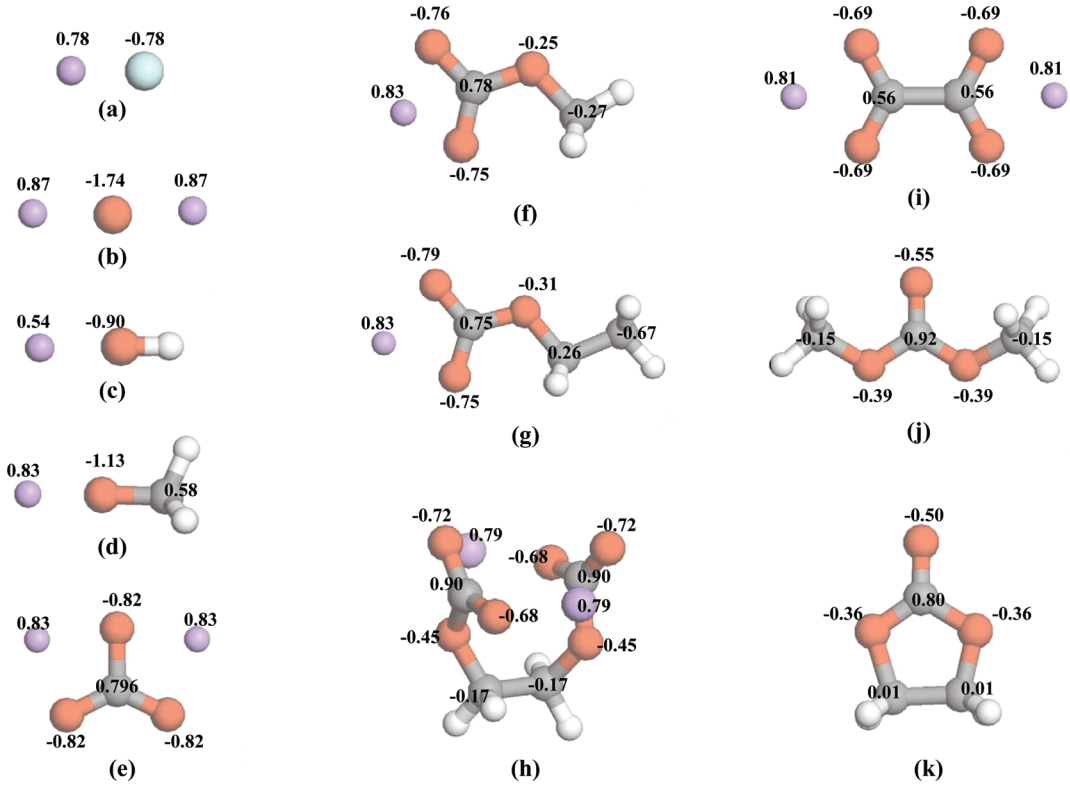

Figure 1. The chemical structures of all molecules studied: (a) lithium fluoride, (b) lithium oxide, (c) lithium hydroxide, (d) lithium methoxide, (e) lithium carbonate, (f) lithium methyl carbonate, (g) lithium ethyl carbonate, (h) dilithium ethylene glycol dicarbonate, (i) lithium oxalate, (j) dimethyl carbonate, and (k) ethylene carbonate. The structures displayed were taken from the optimized structures by energy minimization by DFT calculations. The atomic charges, not shown for the hydrogen atoms, used in computer simulations are also shown by or on the atoms.

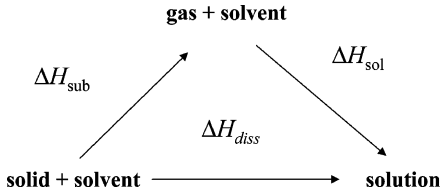

Figure 2. The thermodynamic cycle used for the calculations of the heat of sublimation (ΔH_{sub}), the heat of solution (ΔH_{sol}), and the heat of dissolution (ΔH_{diss}).

have recently reported solubility data for a variety of lithium salts.[36] This provides an opportunity to test and optimize our force field parameters against the experimental data. In this study, we attempt to treat a wide range of salts, including inorganic and organic salts, with either monolithium ion or dilithium ions within the framework of a single potential function. Very few (theoretical) solubility studies have been reported for such a diverse range of salts in organic solvents.

To model ionic solids with reasonable accuracy, it is often desirable to include polarizable potential functions in the force field. However, parametrization of such functions can be time-consuming and requires special expertise. On the other hand, commercial software packages are broadly available and accessible. Materials Studio is a widely used commercial package available from Accelrys, Inc. We will examine the effectiveness of a commercial package dealing with the solubility of ionic solids in this report.

Computation

Figure 1 shows the chemical structures of all the molecules involved in the calculations. Figure 2 illustrates the thermodynamic cycle used in the calculations of the heat of dissolution for each salt in DMC and EC. The heat of sublimation (ΔH_{sub}), the heat of solution (ΔH_{sol}), and the heat of dissolution (ΔH_{diss}) were obtained from the following equations:

$$\Delta H_{sub} = \Delta E_{sub} + RT \quad (1)$$

$$\Delta H_{sol} = \Delta E_{sol} - RT \quad (2)$$

$$\Delta H_{diss} = \Delta H_{sub} + \Delta H_{sol} \quad (3)$$

where ΔE_{sub} is the energy required to bring the salt molecule from the condensed phase to the gas phase, and ΔE_{sol} is the energy required to transfer the same salt molecule from the gas phase to the organic solvent.[48,49] Both ΔE_{sub} and ΔE_{sol} were obtained from the MD simulations. R and T are the gas constant and the absolute temperature, respectively. The temperature was 298 K. The volume change between the salt solution and the liquid (DMC or EC) in the calculation of the heat of solution was assumed to be negligible.[48]

The software package, Materials Studio, used for this study is commercially available from Accelrys, Inc.[50] The force field, using a pairwise potential function, was COMPASS[51] including automatic parameters[52] except for the atomic charges. The atomic charges have been derived from density functional theory (DFT) calculations using the Perdew−Burke−Ernzerhof (PBE) exchange-correlation functional[53,54] through electrostatic potential fitting. The basis set was the double-numerical polarization basis set including one atomic orbital (AO) for each occupied atomic orbital, the second set of valence AOs, *d*-functions for non-hydrogen atoms, and *p*-functions on hydrogen atoms.[55] The atomic charges thus derived for each salt and solvent are shown

TABLE 1: The Heat of Sublimation, the Heat of Solution, and the Heat of Dissolution for Various Lithium Salts (kcal mol^{-1})[a]

	Li_2O[b]	Li_2CO_3[b]	$[LiCO_2]_2$[b]	LiF[b]	$LiOCH_3$	LiOH[b]	$LiOCO_2C_2H_5$	$LiOCO_2CH_3$	LiEDC
					in DMC				
ΔH_{sub}	98.97	88.97	79.95	63.81	50.47	34.41	52.24	49.02	148.40
ΔH_{sol}	−55.72	−56.77	−48.99	−46.64	−45.94	−33.79	−50.44	−52.38	−169.46
ΔH_{dissol}	42.66	31.61	30.37	16.58	3.94	−0.81	1.21	−3.95	−21.65
					in EC				
ΔH_{sub}	98.97	88.97	79.95	63.81	50.47	34.41	52.24	49.02	148.40
ΔH_{sol}	−55.59	−58.49	−66.44	−49.10	−52.06	−39.02	−56.63	−53.68	−161.85
ΔH_{dissol}	42.79	29.89	12.92	14.12	−2.18	−4.02	−4.99	−5.25	−14.04

[a] The temperature was 298 K. [b] The crystal structure was used for the simulations. See the text for the references.

in Figure 1. The van der Waals parameters in COMPASS including automatic parameters are proprietary to Accelrys, Inc. and could not be changed for this study; thus, the original parameters were used. For each salt, 1 ns simulations were run at 298 K under the *NPT* ensemble, under which the number of atoms, the pressure, and the temperature were constant during the simulation, for a cell having a side length of ~20 Å. The exception was LiEDC which required longer simulations, 2 ns, especially in the solid phase, due to its larger molecular size. The average value from several runs was taken as the potential energy used for the heat calculations. The long-range interactions, both van der Waals and electrostatic interactions, were treated by the Ewald summation.[56] Crystal structures were used in the solid simulations of LiOH,[57] LiF,[58] $[LiCO_2]_2$,[59] Li_2CO_3,[60] and Li_2O,[61] and amorphous structures were generated for the others using the Amorphous Cell software package,[62] since no crystallographic data were available.

Results and Discussion

Table 1 lists the heat of dissolution for each salt obtained from the MD simulations, along with the heat of sublimation and the heat of solution in DMC and EC. The heat of dissolution in DMC for the salts ranges from exothermic heats for the organic salts in general to endothermic heats for the inorganic salts in the order of LiEDC < $LiOCO_2CH_3$ < LiOH < $LiOCO_2C_2H_5$ < $LiOCH_3$ < LiF < $[LiCO_2]_2$ < Li_2CO_3 < Li_2O, where the value of the heat went from more negative at the left to more positive at the right. It seems the organic salts are in general more likely to dissolve than the inorganic salts in both DMC and EC. For the results in DMC, this is consistent with our previous experimental observations.[36] The salts tend to dissolve somewhat more in EC than in DMC in general, with an exception for LiEDC, which is addressed later. Our previous work predicted the heat of dissolution for LiEDC to be endothermic.[63] However, the atomic charges in the force field used in the previous work were directly taken from COMPASS and automatic parameters.

A direct comparison with the experimental results is difficult, since the molar concentration was obtained from the solubility measurements,[36] whereas the current calculations presented the heat of dissolution. Yet, a relative comparison may be possible, using the van't Hoff equation. Figure 3 plots the ratio of the molarity on a natural logarithmic scale ($\ln(M_1/M_n)$) against the difference in the heat of dissolution between the salts divided by RT ($-[\Delta H_{diss}(1) - \Delta H_{diss}(n)]/RT$), where 1 and n refer to $LiOCO_2CH_3$ and any other salt, respectively. The comparison was made only for the salts for which experimental data are available. $\ln(M_1/M_n)$) is expressed by a bar including the experimental errors in the figure. The relative positions of $-[\Delta H_{diss}(1) - \Delta H_{diss}(n)]/RT$ with the statistical errors shown by the horizontal line fall within the experimental errors of the

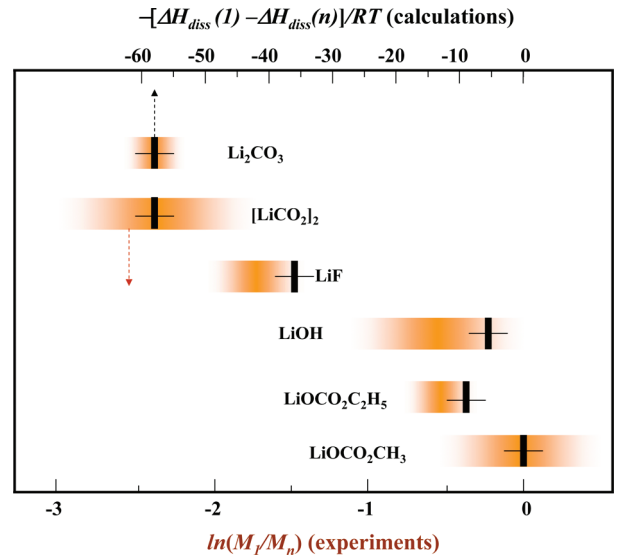

Figure 3. The natural logarithm of M_1/M_n ($\ln(M_1/M_n)$), the lower axis, plotted against $-[\Delta H_{diss}/(1) - \Delta H_{diss}/(n)]/RT$, the upper axis, for the salts for which 1 and n refer to $LiOCO_2CH_3$ and any other salt, respectively. The wide bar represents $\ln(M_1/M_n)$ with the experimental error; the perpendicular line shows $-[\Delta H_{diss}/(1) - \Delta H_{diss}/(n)]/RT$, with the statistical error shown by a thin horizontal line. The solvent was DMC.

corresponding $\ln(M_1/M_n)$, demonstrating that the relative solubility observed by the experiments is reasonably well reproduced by the calculations. The relative solubility of such a wide range of lithium salts including inorganic and organic salts with either dilithium or monolithium salt has not previously been reproduced within the framework of the same force field potential function.

Experimental data is scarcely available for comparison with the calculations. Table 2 summarizes the comparison with the available literature values, the density and the heat of vaporization for DMC[64] and EC,[65] and also the heat of sublimation for LiF,[66] all of which are reasonably reproduced by the calculations. One could argue that the errors associated with both the heat of sublimation and the heat of solution by our calculations may be canceled out, since the heat of dissolution is a summation of ΔH_{sub} and ΔH_{sol}. However, the comparison of ΔH_{sub} with the available experimental data does not support the claim, at least for LiF. Still, the calculations are only meant to be compared to the experiments qualitatively, since they only give the heat of dissolution; the entropy is difficult to calculate for the systems studied. As for the crystallographic data for those salts for which the crystal structure was used for the solid simulations, the agreement with the experimental data is not as satisfactory. It should be noted that only atomic charges were modified in the simulations; the van der Waals parameters were used directly from COMPASS and automatic parameters due

TABLE 2: Comparisons of Calculations and Experimental Data[a]

	DMC	EC
density	1.06 ± 0.02	1.30 ± 0.02
g cm^{-3}	(1.07[b])	(1.32[b])
heat of vaporization	9.47 ± 0.48	12.04 ± 0.42
kcal mol^{-1}	(9.26[c])	(13.45[d])

	LiF	Li_2O	Li_2CO_3	$[LiCO_2]_2$	LiOH
heat of sublimation	63.81				
kcal mol^{-1}	(64.59[e])				
lattice constant	3.88 Å	4.48 Å	$a/b/c$ = 8.01/4.64/5.85 Å	$a/b/c$ = 5.27/2.98/5.62 Å	$a/b/c$ = 6.56/7.46/2.62 Å
	(4.02[f])	(4.61[g])	β = 114.79°	$\alpha/\beta/\gamma$ = 98.43/97.92/78.77°	β = 102°
			($a/b/c$ = 8.36/4.97/6.19 Å	($a/b/c$ = 5.66/3.36/5.97 Å	($a/b/c$ = 7.37/8.26/3.19 Å
			β = 114.79°[h])	$\alpha/\beta/\gamma$ = 98.43/97.92/78.77°[i])	β = 110.18°[j])

[a] The experimental data is in the parentheses. [b] Taken from ref 67. [c] Taken from ref 64. [d] Taken from ref 65. [e] Taken from ref 66. [f] Cubic, taken from ref 58. [g] Cubic, taken from ref 61. [h] Monoclinic, taken from ref 60. [i] Triclinic, taken from ref 59. [j] Monoclinic, taken from ref 57.

TABLE 3: The Number of the Carbonyl and the Ether Oxygens of the Solvent in the First Shell of the Li^+ Solvation[a]

DMC									
oxygen	Li_2O	Li_2CO_3	$[LiCO_2]_2$	LiF	$LiOCH_3$	LiOH	$LiOCO_2C_2H_5$	$LiOCO_2CH_3$	LiEDC
carbonyl oxygen	1.82	2.08	2.06	2.80	2.56	2.11	2.40	2.50	2.31
ether oxygen	0.30	0.05	0.16	0.04	0.36	0.61	0.11	0.03	0.20
total	2.12	2.13	2.22	2.84	2.92	2.72	2.51	2.53	2.51
EC									
oxygen	Li_2O	Li_2CO_3	$[LiCO_2]_2$	LiF	$LiOCH_3$	LiOH	$LiOCO_2C_2H_5$	$LiOCO_2CH_3$	LiEDC
carbonyl oxygen	1.82	2.07	2.53	2.84	2.64	2.12	2.76	2.81	1.90
ether oxygen	0.50	0.04	0.21	0.32	0.44	0.75	0.32	0.14	0.0
total	2.32	2.11	2.74	3.16	3.08	2.87	3.08	2.95	1.9

[a] Obtained from integration of the pair distribution function for Li^+ and the carbonyl oxygen or the ether oxygen up to 3 Å from Li^+. The values for the dilithium salts were averaged over the two lithium cations.

to the constraint described in the Computation section. With a judicious modification of the van der Waals parameters, we expect that the agreement with the experimental crystallographic data could be improved, but on the basis of Figure 3, we believe the calculated relative solubility is valid.

A variety of solvents are currently used in lithium ion battery electrolytes, including cyclic carbonates and linear carbonates, among others. It is thus of particular interest to examine the solubility of salt components found in SEI films in other solvents. EC is one of the most popular solvents used in the lithium ion battery electrolytes. Our computer simulations have shown that the heat of dissolution is generally somewhat more exothermic (or less endothermic) for the salts in EC than in DMC. One reason may be that EC is a more polar solvent than DMC. The dielectric constant of EC is 89.6, whereas that for DMC is 3.12 at room temperature.[67] It is of interest to note that after cycling, cell capacity recovery has been observed once the anode electrode was rinsed in water, which has a dielectric constant of 80.2 at room temperature.[12,68]

In addition, we suspect that the molecular shape of the solvent may affect the solubility of the salt. For example, EC is a rather compact molecule, having a cyclic structure, whereas DMC is a chain molecule having two terminal methyl groups with the C═O bond perpendicular to the chain axis (see Figure 1). Since solvation of the lithium cation occurs primarily with the C═O dipole of the carbonate solvent pointing at the cation, as shown below, the differences in the molecular structures between the solvents may result in a different accessibility of the solvent to the cation for solvation. The lithium cation can also be solvated by the ether oxygen of the carbonate solvent. Due to the cyclic structure's having its ethylene groups pointing away from the lithium cation, EC may have better accessibility to the cation than DMC, whose methyl groups can point toward the cation. On the other hand, a DMC molecule's contact with its neighboring solvent molecules through the flexible terminal groups may become more repulsive, and it gets increasingly crowded around the lithium ion as the DMC molecule tries to approach the cation. By extending this argument, it may follow that salts may be less soluble, as compared with in DMC, in diethyl carbonate (DEC) which has a longer terminal group than DMC. Still, the above discussions remain only speculation.

Table 3 summarizes the differences in the Li^+ solvation structure between that in DMC and in EC. The table lists the number of the carbonyl oxygens and ether oxygens of the solvent molecules within the first solvation shell of the Li^+ ion in each solvent. They were obtained through integration of the pair distribution function (PDF),

$$g(r) = \frac{1}{4\pi\rho r^2}\frac{dN(r)}{dr} \tag{4}$$

where ρ is the atom number density, r is the interatomic distance between the Li^+ ion and either the carbonyl oxygen or the ether oxygen atom, and N is the number of oxygen atoms within the distance r. The integration of the PDF was performed up to 3 Å, by which point the first peak disappeared in the most distribution functions. Figure 4 displays typical PDFs for pairs both in DMC and in EC. Figure 4a shows the PDF for the Li^+−carbonyl oxygen pair in DMC, where a sharp peak appears around 2 Å, corresponding to the nearest carbonyl oxygen atoms coordinating the Li^+ ion. The only other peak is broad and appears beyond 6 Å, which corresponds to the carbonyl oxygen atoms in the second solvation shell. The dominant first peak in the PDF demonstrates strong interactions between the Li^+ ion and the carbonyl oxygen atoms of DMC surrounding the ion.

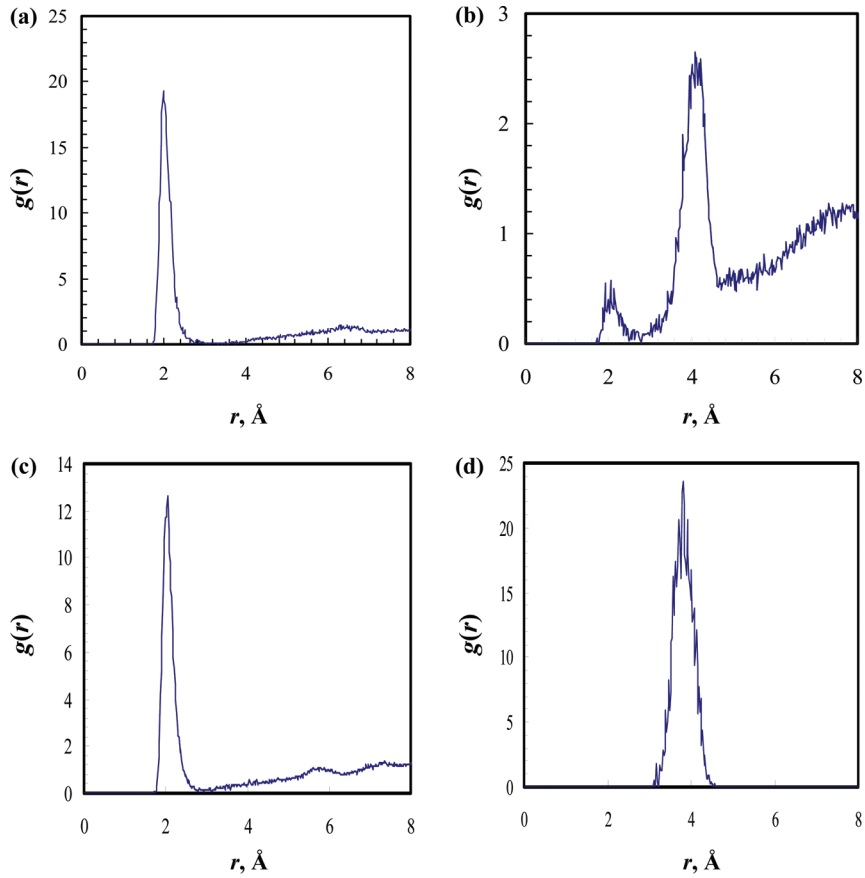

Figure 4. Pair distribution functions (g(r)) for (a) the Li^+−carbonyl oxygen (DMC) pair, (b) the Li^+−ether oxygen (DMC) pair, (c) the Li^+−carbonyl oxygen (EC), and (d) the Li^+−ether oxygen of EC.

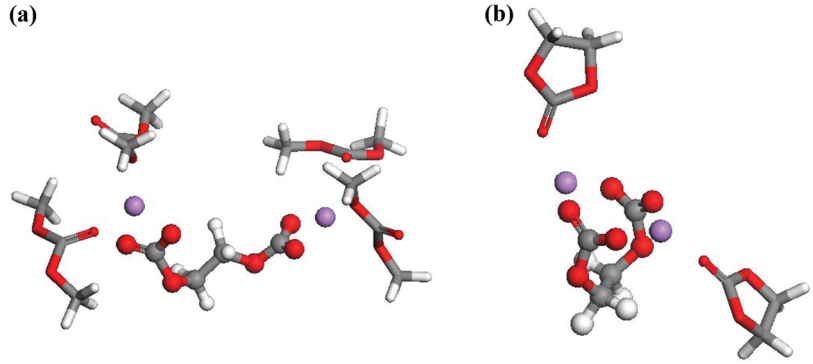

Figure 5. Snapshots taken from MD simulations: (a) LiEDC in DMC and (b) LiEDC in EC.

The Li^+−ether oxygen PDF in DMC, in Figure 4b, on the other hand, has two clear peaks around 2 and 4 Å, which correspond to the ether oxygen of DMC nearest to Li^+ and the other ether oxygen in the same or the adjacent DMC molecule, respectively. The first peak at around 2 Å clearly indicates that some ether oxygens directly solvate the Li^+ ion. The reason for the second peak, higher than the first, is that the contribution to the second peak also includes those from the ether oxygens belonging to the adjacent DMC molecules, which solvate the Li^+ ion through the carbonyl oxygens.

In sharp contrast, the Li^+−ether oxygen PDF in EC in Figure 4d shows only a single peak around 4 Å, which is due to the ether oxygen of EC molecules that solvate the lithium ions through their carbonyl oxygens. A compact, closed conformation of LiEDC in EC, shown in Figure 5b, gives limited accessibility to the solvent. This conformation allows only the carbonyl oxygen to access the lithium ion, since this orientation minimizes the van der Waals overlap between the LiEDC molecule and the solvent molecules. The limited accessibility of the solvents also removes the ether oxygens of EC up to 10 Å from the lithium ion, which is the reason no peak appears in Figure 4d.

The results in Table 3 indicate that the carbonyl oxygen directly solvates Li^+ more than the ether oxygen. From the simulation trajectories, it was occasionally observed that both a carbonyl and ether oxygen of the same solvent molecule simultaneously solvate Li^+, but such occurrences were rare. For the most part, the carbonyl oxygens and the ether oxygens within 3 Å from the lithium ion belonged to different solvent molecules. Thus, the total number of the carbonyl and ether oxygens in the fourth row of Table 3 can be considered as the total solvation number in the first shell of the lithium salt. It is shown that the solvation number is around 3, except for Li_2CO_3, Li_2O, and $[LiCO_2]_2$, for which the number is around 2, at least in DMC. The solvation number of 3.7 for Li^+ has been recently reported

by Yamada et al.[69] With one solvation site still occupied by the anion counterpart, the solvation number of around 3 seems consistent with the crystallographic data. As to Li_2CO_3, Li_2O, and $[LiCO_2]_2$, these salts have two lithium ions for solvation, which may bring the solvent molecules too close to one another to have a solvation number of 3. The high negative charges on the oxygen may be at work as well, pushing the solvent molecules away from the lithium ion. The solvation number for $[LiCO_2]_2$ increases to almost 3 in EC, which suggests a higher accessibility of EC molecules than that of DMC. The results in Table 3 demonstrate that in general, the solvation number in EC is higher than in DMC, except for LiEDC, which will be discussed below. The higher solvation numbers of the salts in EC than in DMC correlate reasonably well with the somewhat more exothermic heats of dissociation for the salts in EC relative to those in DMC.

LiEDC is obviously an exception to the general trend that the other salts exhibit for solubility in DMC relative to that in EC. The conformation of LiEDC in both solvents was examined from the MD trajectories. Figure 5 illustrates the solvation of LiEDC in each solvent taken from the MD trajectories. As mentioned above, in EC, LiEDC maintains a compact, closed conformation, which is the most stable found in the gas phase, as well. This conformation may be favorable entropically in EC, given the compact, closed structure of the EC molecules. The two lithium ions are shared by both terminal carbonate groups, keeping the lithium ions with the anion from accessing for solvation. In DMC, on the other hand, LiEDC transforms itself to an open conformation, separating the two lithium ions from one another, further away from the opposite side of the terminal carbonate group. The conformation of LiEDC in DMC is believed to be also entropically driven, since DMC is a chain molecule, as well. Now each lithium ion is more exposed to the solvent, allowing the solvent access, becoming more prone to dissolution. In fact, Table 3 indicates that the solvation number for the lithium ion of LiEDC is higher in DMC than in EC. It should be noted, however, that the simulations in EC were performed at 298 K to compare without the temperature effect on the results in DMC obtained from simulations at 298 K. Hence, the results in EC are presented only for theoretical comparisons to those in DMC, since the melting point of EC is 313 K. We observed, however, that LiEDC remained in a closed conformation at 313 K, as well.

As to the relative solubility among the salts, its rationalization seems rather straightforward in terms of the electrostatic interactions and the crystal molecular packing. The electrostatic interactions in the current modeling framework are controlled through Coulombic interactions by the atomic charges assigned to each atom, shown in Figure 1. Table 1 suggests a general correlation between the heat of sublimation of the salts and their atomic charges, especially the oxygen charges. For example, a relevant comparison can be made between the oxygen charge for $LiOCO_2CH_3$ ($-0.76e$, $-0.75e$, or $-0.25e$) and that for Li_2O ($-1.74e$) and their corresponding heat of sublimation: 49.02 and 98.97 kcal mol^{-1}, respectively. In fact, the heat of sublimation for dilithium salts such as Li_2O is generally higher than that for the monolithium salts because two lithium ions in Li_2O induce higher polarization in the molecule, resulting in the higher atomic charges. In fact, Li_2O has one of the highest values for the heat of sublimation among the salts studied here.

On the other hand, the oxygen of $LiOCH_3$, a monolithium salt, also has a rather large charge, $-1.13e$, yet its heat of sublimation is only the second smallest among the salts studied: 50.47 kcal mol^{-1}. We suspect this is due primarily to the molecular packing of $LiOCH_3$ in the crystal lattice, which may not be as closely packed as Li_2O or LiF, because of the methyl group of $LiOCH_3$. The methyl group may prevent a close molecular packing. Both Li_2O and LiF are linear molecules, on the other hand, more likely to pack themselves densely in the lattice. For the same reason, lithium oxalate, having a plane structure (see Figure 1i) allowing tight molecular packing, has a high heat of sublimation, 79.95 kcal mol^{-1}, despite its not so large charge, $-0.69e$, for the oxygen. As for LiEDC, its atomic charges are not as large as those of Li_2O, yet it has the largest heat of sublimation, 148.40 kcal mol^{-1}, which contradicts the discussion above. We suspect that this is simply a result of the large molecular size, the largest among the salts, having many interacting points, giving rise to stronger interactions between the molecules in the solid. The size of the molecule has been used as one of the molecular descriptors to predict heats of sublimation for a large number of molecules.[70] As to the process of dissolving a salt molecule into a solvent, the separation of the lithium from the anion counterpart of the salt is the primary driving force for dissolution. Here, again, the electrostatic interactions play a dominant role. There seems to be a correlation between the atomic charges and the heat of solution for the salts.

Crystal structures were not used for some of the salts in the simulations, since crystallographic data are available only for LiOH, LiF, $[LiCO_2]_2$, Li_2CO_3, and Li_2O.

Amorphous structures were used for other salts. The effect of using a crystal structure on the heat of dissolution was examined for those salts whose crystal structures are known. For amorphous simulations, to avoid a system's being trapped in a shallow potential well, the cell was first heated to 600 K, then gradually cooled to 298 K, followed by a 1 ns simulation at the same temperature. For LiOH, LiF, $[LiCO_2]_2$, Li_2CO_3, and Li_2O, the heat of dissolution obtained from such amorphous simulations was 1.24, 7.45, 8.49, 23.94, and 80.02 kcal mol^{-1}, respectively. The differences from those obtained from the crystal simulations ranged from 0.14 kcal mol^{-1} for LiOH to 37.38 kcal mol^{-1} for Li_2O. Yet, the order for dissolution either in DMC or EC was not altered. We note that some studies have found amorphous regions in SEI films.[13] Experimental solubility data for EC is not available for a comparison with our calculated results. Still, we note that the current force field reproduced the thermodynamic data for both EC and DMC fairly well, as is shown in Table 2.

A pairwise potential function has been used as the force field in the current simulations, whereas a polarizable function is often used to model ionic solids.[39,42,71] The force field used here is based on a pairwise potential function without many-body-effect terms. Yet, at least, the heat of sublimation for LiF was reasonably reproduced by our calculations. Still, the treatment of the isoelectronic F^- may be less problematic in the force field calculations than Li_2O having the high delocalization of the second electron of the outermost shell O^{2-}, inducing a nonspherical electron density around the oxygen. For example, the Cauchy violation for Li_2O is known to be difficult to reproduce using pairwise potential functions,[39] yet some known properties of the salts such as Li_2O have been well-reproduced by pairwise potentials.[44] Gale has suggested that for many ionic materials, it is often sufficient to include only the two-body term in the potential function.[37] However, for quantitative discussions on salts such as Li_2O, the inclusion of the polarizable potential function is obviously favored.

Conclusion

The relative solubility among a wide range of lithium salts, all of which are well-known SEI components, has for the first time been reasonably well reproduced in DMC by computer simulations using a force field with DFT-derived atomic charges. The heats of dissolution for the organic salts were found to be either exothermic or slightly endothermic, whereas all the inorganic salts showed endothermic heats of dissolution. The heat of dissolution became more exothermic in the following order in DMC: LiEDC > $LiOCO_2CH_3$ > LiOH > $LiOCO_2C_2H_5$ >$LiOCH_3$ > LiF > $[LiCO_2]_2$ > Li_2CO_3 > Li_2O.

The heats of dissolution for the same salts were also calculated in EC. It was found that the salts tended to dissolve more in EC than in DMC, except for LiEDC. Our analysis suggests that not only does the polarity of the solvent influence the solubility of the salt, but also the size and shape of the solvent molecule may play an important role. Only LiEDC was less soluble in EC than in DMC, due to its conformation, which may obstruct the Li^+ dissociation. The solubility of each salt has been discussed in terms of the electrostatic interactions and the molecular packing. We find that in general, the larger the size of the salt molecule is, the more soluble it becomes; namely, a large size of the salt molecule may promote delocalization of the electrons over the molecule, leading to weaker electrostatic interactions with atoms in the neighboring molecules in the solid and giving rise to a lower heat of sublimation. Salts having a linear or planar molecular shape promoting an enhanced molecular packing in a crystal lattice tend to dissolve less than salts having bulky groups or flexible chains. Furthermore, a compact molecular shape of the solvent, such as EC, may help solvate the lithium ion, resulting in more heat of solution.

We have demonstrated the effective use of a commercial software package for modeling the relative solubility of a wide range of lithium salts in organic solvents with a combination of atomic charge adjustments from DFT calculations. Still, it should be noted that the discussion presented here should be taken only as qualitative, since the van der Waals parameters were not optimized and, in addition, a pairwise potential function for the salts was used for the force field. More rigorous parametrization including a polarizable function should not only provide a better agreement with the crystallographic data for some of the salts studied here, but also allow quantitative discussions on the salt solubility.

Acknowledgment. The authors thank Drs. Alexander Goldberg, Jian-Jie Lian, Matthew Hat, and George Fitzgerald of Accelrys, Inc. for their very helpful comments and advice.

References and Notes

(1) Peled, E.; Goloditsky, D.; Penciner, D. J. In *Handbook of Battery Materials*; Besenhard, J. O., Ed.; Wiley-VCH.: Weinheim, 1999; p 419.
(2) Andersson, A.; Edström, K.; Thomas, J. O. *J. Power Sources* **1999**, *81*, 8.
(3) Jean, M.; Chausse, A.; Messina, R. *Abstract 146*; 192nd Electrochem. Soc. Meeting Paris, 1997.
(4) Vetter, J.; Novák, P.; Wagner, M. R.; Veit, C.; Moller, K. C.; Besenhard, J. O.; Winter, M.; Wohlfahrt-Mehrens, M.; Vogler, C.; Hmmouche, A. *J. Power Sources* **2005**, *147*, 269.
(5) Du Pasquier, A.; Disma, F.; Bowmer, T.; Gozdz, A. S.; Amatucci, G.; Tarascon, J.-M. *J. Electrochem. Soc.* **1998**, *145*, 472.
(6) Safari, M.; Morcrette, M.; Teyssot, A.; Delacourt, C. *J. Electrochem. Soc.* **2009**, *156*, A145.
(7) Darling, R.; Newman, J. *J. Electrochem. Soc.,* **1998**, *145*, 990.
(8) Ramasamy, R. P.; Lee, J. W.; Popov, B. N. *J. Power Sources* **2007**, *166*, 266.
(9) Ramadass, P.; Haran, B. S.; Gomadam, P. M.; White, R.; Popov, B. N. *J. Electrochem. Soc.* **2004**, *151*, A196.
(10) Geniès, S.; Brun-Buisson, D.; Wu, Y.-F.; Mattera, F.; Merten, J. *Abstract 1280*; 214th Electrochemical Society Meeting, Honolulu, 2008.
(11) Abraham, D. P.; Knuth, J. L.; Dees, D. W.; Bloom, I.; Christophersen, J. P. *J. Power Sources* **2007**, *170*, 465.
(12) Broussely, M.; Biensan, P.; Bonhomme, F.; Blanchard, P.; Herreyre, S.; Nechev, K.; Staniewicz, R. J. *J. Power Sources* **2001**, *97*−*98*, 13.
(13) Leroy, S.; Blanchard, F.; Dedryvere, R.; Martinez, H.; Carre, B.; Lemordant, D.; Gonbeau, D. *Surf. Interface Anal.* **2005**, *37*, 773.
(14) Aurbach, D.; Ein-Eli, Y.; Markovsky, B.; Zaban, A.; Luski, S.; Carmeli, Y.; Yamin, H. *J. Electrochem. Soc.* **1995**, *142*, 2882.
(15) Aurbach, D.; Levi, M. D.; Levi, E.; Schechter, A. *J. Phys. Chem. B* **1997**, *101*, 2195.
(16) Leroy, S.; Blanchard, F.; Dedryvere, R.; Martinez, H.; Carre, B.; Lemordant, D.; Gonbeau, D. *Elecrochim. Acta* **2008**, *53*, 3539.
(17) Augustsson, A.; Herstedt, M.; Guo, J.-H.; Edstrom, K.; Zhuang, G. V.; Ross, P. N., Jr.; Rubensson, J.-E.; Nordgren, J. *Phys. Chem. Chem. Phys.* **2004**, *6*, 4185.
(18) Cheng, H.; Zhu, C.; Lu, M.; Yang, Y. *J. Power Sources* **2007**, *173*, 531.
(19) Zhang, S. S.; Xu, K.; Jow, T. R. *Electrochim. Acta* **2006**, *51*, 1636.
(20) Zhuang, G. V.; Ross, P. N. *Electrochem. Solid State Lett.* **2003**, *6*, A136.
(21) Zhao, L.; Watanabe, I.; Doi, T.; Okada, S.; Yamaki, J. *J. Power Sources* **2006**, *161*, 1275.
(22) Fong, R.; Von Sacken, U.; Dahn, J. R. *J. Electrochem. Soc.* **1990**, *137*, 2009.
(23) Aurbach, D.; Markovsky, B.; Weissman, I.; Levi, E.; Ein-Eli, Y. *Electrochim. Acta* **1999**, *45*, 67.
(24) Dedryvere, R.; Leroy, S.; Martinez, H.; Blanchard, F.; Lemordant, D.; Gonbeau, D. *J. Phys. Chem. B* **2006**, *110*, 12986.
(25) Aurbach, D.; Zinigrad, E.; Cohen, Y.; Teller, H. *Solid State Ionics* **2002**, *148*, 405.
(26) Zhuang, G. V.; Yang, H.; Blizanac, B.; Ross, P. N. *Electrochem. Solid State Lett.* **2005**, *8*, A441.
(27) Naejus, R.; Lemordant, D.; Coudert, R.; Willimann, P. *J. Fluorine Chem.* **1998**, *90*, 81.
(28) Aurbach, D.; Zaban, A.; Gofer, Y.; Ein-Eli, Y.; Weissman, I.; Chusid, O.; Abramson, O. *J. Power Sources* **1995**, *54*, 76.
(29) Ein-Eli, Y.; Markovsky, B.; Aurbach, D.; Carmeli, Y.; Yamin, H.; Luski, S. *Electrochim. Acta* **1994**, *39*, 2559.
(30) Richard, M. N.; Dahn, J. R. *J. Electrochem. Soc.* **1999**, *146*, 2068.
(31) Chusid, O.; Ein-Eli, Y.; Aurbach, D.; Babai, M.; Carmeli, Y. *J. Power Sources* **1993**, *43*−*44*, 47.
(32) Ota, H.; Sakata, Y.; Inoue, A.; Yamaguchi, S. *J. Electrochem. Soc.* **2004**, *151*, A1659.
(33) Ota, H.; Sakata, Y.; Wang, X.; Sasahara, J.; Yasikawa, E. *J. Electrochem. Soc.* **2004**, *151*, A437.
(34) Andersson, A. M.; Edsröm, K. *J. Electrochem. Soc.* **2001**, *148*, A1100.
(35) Xu, K.; Zhang, S.; Jow, T. R. *Electrochem. Solid State Lett.* **2003**, *6*, A117.
(36) Tasaki, K.; Goldberg, A.; Lian, J.-J.; Walker, M.; Timmons, A.; Harris, S. J. *J. Electrochem. Soc.* **2009**, *156*, A1019.
(37) Gale, J. In *Handbook of Materials Modeling*; Yip, S., Ed.; Springer: The Netherlands, 2005; p 479.
(38) Wilson, M.; Jahn, S.; Madden, P. A. *J. Phys.: Condens. Matter* **2004**, *16*, S2795.
(39) Chadwick, A. V.; Flack, K.; Strange, J. H.; Harding, J. H. Proc. 6th Int. Conf. on Solid State Ionics, Garmisch-Partenkirchen, Fed. Rep. Germany, Sept. 6−11, 1987.
(40) Rodeja, J. G.; Meyer, M.; Hayoun, M. *Modell. Simul. Mater. Sci. Eng.* **2001**, *9*, 81.
(41) Jacobs, P. W. M.; Vernon, M. L. *J. Chem. Soc., Faraday Trans.* **1990**, *86* (8), 1233.
(42) Gavartin, J. L.; Catlow, C. R. A.; Shluger, A. L.; Varaksin, A. N.; Kolmogorov, Y. N. *Modell. Simul. Mater. Sci. Eng.* **1992**, *1*, 29.
(43) Bush, T. S.; Gale, J. D.; Catlow, C. R. A.; Battle, P. D. *J. Mater. Chem.* **1994**, *4* (6), 831.
(44) Fracchia, R. M.; Barrera, G. D.; Allan, N. L.; Barron, T. H. K.; Mackrodt, W. C. *J. Phys. Chem. Solids* **1998**, *59*, 435.
(45) Gavartin, J. L.; Shluger, A. L.; Catlow, C. R. A. *J. Phys.: Condens. Matter* **1993**, *5*, 7397.
(46) Zhou, L. X.; Hardy, J. R.; Cao, H. Z. *Solid State Commun.* **1996**, *99*, 637.
(47) Habasaki, J. *Mol. Phys.* **1990**, *69*, 115.
(48) Jorgensen, W. L.; Madura, J. D. *J. Am. Chem. Soc.* **1983**, *105*, 1408.
(49) Lousada, C. M.; Pinto, S. S.; Lopes, J. N.C.; da Piedade, M. F. M.; Diogo, H. P.; da Piedade, M. E. M. *J. Phys. Chem. A* **2008**, *112*, 2977.
(50) *Materials Studio, V4.3*, Accelrys, Inc.: 10188 Telesis Ct., Suite 100, San Diego, CA 92121.
(51) Sun, H. *J. Phys. Chem. B* **1998**, *102*, 7338.
(52) Eichinger, B. E.; Rigby, D.; Stein, J. *Polymer* **2002**, *43*, 599.

(53) Perdew, J. P.; Burke, K.; Ernzerhof, M. *Phys. Rev. Lett.* **1996**, *77*, 3865.
(54) Perdew, J. P.; Burke, K.; Ernzerhof, M. *Phys. Rev. Lett.* **1997**, *78*, 1396.
(55) Sadhukhan, S.; Munoz, D.; Adamo, C.; Scuseria, G. E. *Chem. Phys. Lett.* **1999**, *306*, 83.
(56) Ewald, P. *Ann. Phys.* **1918**, *54*, 519.
(57) Alcock, N. W. *Acta Crystallogr.* **1971**, *B27*, 168.
(58) Thewlis, J. *Acta Crystallogr.* **1955**, *8*, 36.
(59) Pedersen, B. F. *Acta Chem. Scand.* **1969**, *23*, 1871.
(60) Idemoto, Y.; Richardson, J. W.; Koura, N.; Loong, C.-K. *J. Phys. Chem.* **1998**, *59*, 363.
(61) Shunk, F. A. *Consitution of Binary Alloys*, 2nd Suppl.; McGraw-Hill: New York, 1969.
(62) *Amorphous Cell*; Accelrys, Inc.: 10188 Telesis Ct., Suite 100, San Diego, CA 92121.
(63) Tasaki, K. *J. Phys. Chem. B* **2005**, *109*, 2920.
(64) Steele, W. V.; Chirico, R. D.; Knipmeyer, S. E.; Nguyen, A. *J. Chem. Eng. Data* **1997**, *42*, 1008.
(65) Hong, C. S.; Wakslak, R.; Finston, H.; Fried, V. *J. Chem. Eng. Data* **1982**, *27*, 146.
(66) Chase, M. W., Jr.; Davis, C. A.; Downy, J. R., Jr.; Frurip, D. J.; McDonald, R. A.; Syverud, A. N. *JANAF Thermochemical Tables*, 3rd ed.; National Bureau of Standards: Washington, DC, 1985.
(67) Linden, D. *Handbook of Batteries*, 2nd ed.; MaGraw-Hill: New York, 1995; p 36.14.
(68) Archer, D. G.; Wang, P. *J. Phys. Chem. Ref. Data* **1990**, *19*, 371.
(69) Yamada, Y.; Koyama, Y.; Abe, T.; Ogumi, Z. *J. Phys. Chem. C* **2009**, *113*, 8948.
(70) Gharagheizi, F. *Thermochim. Acta* **2008**, *469*, 8.
(71) Wilson, M.; Exner, M.; Huang, Y. M.; Finnis, M. W. *Phys. Rev. B* **1996**, *54*, 683.

JP100013H